CORROSION BEHAVIOR OF IRON AND NICKEL BASE ALLOYS UNDER SOLID OXIDE FUEL CELL EXPOSURE CONDITIONS

M. Ziomek-Moroz, G.R. Holcomb, B.S. Covino, Jr., S.J. Bullard
U.S. Department of Energy, Albany Research Center
1450 Queen Avenue, SW
Albany, OR 97321

ABSTRACT

Topography and phase composition of the scales formed on commercial ferritic stainless steels and experimental low CTE nickel-based alloys were studied in atmospheres simulating solid oxide fuel cell (SOFC) environments. The materials were studied under dual environment conditions with air on one side of the sample and carbon monoxide on the other side at 750^{o}C. Surface characterization techniques, such as scanning electron microscopy and X-ray diffraction analysis were used in this study.

INTRODUCTION

Hydrogen is the primary gaseous fuel in fuel cells and is used in the following major fuel cells:[1]

Alkaline Fuel Cells (AFC)
Phosphoric Acid Fuel Cells (PAFC)
Proton Exchange Membrane Fuel Cells (PEMFC)
Molten Carbonate Fuel Cells (MCFC)
Solid Oxide Fuel Cells (SOFC)

One of the main advantages of SOFC over other types of fuel cells is their ability to handle more convenient hydrocarbon fuels while other types of fuel cells must rely on a clean supply of hydrogen for their operation.[2] At present, the most common fuels are natural gas and coal. One of the means of

producing hydrogen from fossil fuels is steam reforming of hydrocarbons. The reaction for steam reforming can be formulated for methane (Eq.) as the main component of natural gas:[3]

$$CH_4 + H_2O = CO + 3H_2 \quad (1)$$

Mixtures of CO and H_2 produced from carbon-containing feedstock are called synthetic gas or syngas. A further process involves the conversion of CO in the water-gas shift reaction (Eq. 2):

$$CO + H_2O = CO_2 + H_2 \quad (2)$$

A typical steam reformed natural gas reformate is presented in Table 1.

TABLE 1
TYPICAL STEAM REFORMED NATURAL GAS REFORMATE COMPOSITION

Specie	Reformer Effluent, Mole %	Shifted Reformate, Mole %
H_2	46.3	52.9
CO	7.1	0.5
CO_2	6.4	13.1
CH_4	2.4	2.4
N_2	0.8	0.8
H_2O	37.0	30.4
Total	100.0	100.0

During SOFC operations, H_2, CO, and CH_4 will be oxidized at the anode according to the following oxidation reactions:[2]

$$H_2 + O^{2-} \rightarrow H_2O + 2e \quad (3)$$
$$CO + 2O^{2-} \rightarrow CO_2 + 2e \quad (4)$$
$$CH_4 + 4O^{2-} \rightarrow CO_2 + 2H_2O + 8e \quad (5)$$

An interconnect, which connects individual cells and acts as a gas separator, is exposed to cathode gas (usually air) on one side and to anode gas on the other side. The composition of the anode side depends upon the type of fuel used, e.g., H_2, CH_4, CO/H_2.[2] Significant progress in reducing the operating temperature of SOFC from ~1000°C to ~800°C may allow for a shift from costly ceramic interconnects to less expensive metallic interconnects. The most promising metallic materials are chromia scale forming alloys since they fulfill the technical and economical requirements.[4] They have the advantage of higher electronic conductivity, easer fabricability, and lower cost than ceramic materials. Results of the oxidation behavior of ferritic and nickel-based alloys in moist hydrogen within temperature range 650-800ºC have been reported.[5,6] Also, results on the corrosion behavior of selected commercial iron-base and nickel-base alloys exposed to carburizing gases at ~600 ºC have been reported. Some of the investigated alloys underwent accelerated corrosion known as metal dusting.[7]

Literature data indicate that in CO/CO_2 gaseous environments, metallic materials that gain their corrosion resistance due to formation of Cr_2O_3, could form stable chromium carbides.[8,9] The chromium carbide formation causes depletion of chromium in these alloys. If the carbides oxidize, they form non-protective scales.

Considering a potential detrimental effect of CO on iron- and nickel- base alloy stability, determining corrosion performance of metallic interconnect candidates in CO at SOFC operating temperatures is a must. Therefore, this paper describes the corrosion behavior of metallic materials,

namely a ferritic stainless steel containing 22 wt. % Cr (Fe-22Cr) and two experimental nickel - base alloys, J1 without manganese [10,11] and J5 with manganese [12,13], simultaneously exposed to air on one side and carbon monoxide on the other side at 750°C for 200 h.

EXPERIMENTAL PROCEDURE

Corrosion experiments were performed on the following materials: J1, J5, and Fe-22Cr. The chemical composition of the investigated materials determined by wet chemistry is shown in Table 2.

TABLE 2
CHEMICAL COMPOSITION OF J1, J5, AND Fe-22Cr (Wt. %)

Alloy	Mo	Ni	Fe	Mn	Cr	Al	Y	Ti	La
J1	17.85	Balance	0.040	0	12.07	0.79	N.D.	1.1	N.D.
J5	22.17	Balance	0.027	0.50	12.50	0.038	0.043	1.02	N.D.
Fe-22Cr	0.002	0.32	Balance	0.45	22.33	0.13	N.D.	0.1	0.1

J1[10,11] is an experimental Ni-base alloy with low coefficient of thermal expansion (CTE). The composition of J1 is based based on Mitsubishi all LTES700, which was developed for advanced (700ºC) steam turbine applications. J5[12,13] is a novel low CTE nickel-based alloy developed by the U.S. Department of Energy, Albany Research Center for SOFC applications. The nickel- based alloys were prepared at the U.S. Department of Energy, Albany Research Center. Fe-22Cr is low CTE commercial ferritic stainless, Crofer 22 APU, developed for SOFC applications by Forschungszentrum Julich and commercialized by ThyssenKrupp VDM. All experiments were performed on materials as received, i.e., no additional heat treatment was performed.

Samples were planar round pieces approximately 2.4 cm (0.943") in diameter and 1mm in thickness. Before each test, the samples were polished with 600 grit SiC paper and ultrasonically cleaned in acetone. After degreasing the surfaces, the samples were mounted onto a dual environment fixture[14] and installed inside the furnace. The samples were simultaneously exposed to a dual environment, with CO on one side and air on the other side, for 200 h at 750 °C.

Scale reaction products were determined by X-ray diffraction (XRD). Surface microstructure and topography of the scale was characterized by scanning electron microscopy (SEM). Chemical composition of the scale reaction products was determined by wavelength dispersive energy X-ray (WDX) spectroscopy.

RESULTS AND DISSCUSION

Figure 1 shows SEM (secondary electrons) micrographs of the scale formed on the J1 sample in the dual environment with one surface oxidized in air and the other surface in CO. The surface exposed to air is covered uniformly with cubic-and tetragonal-like grains. The surface exposed to CO is covered uniformly with whisker-like scale. The phases determined by XRD in the scale formed on the air side are $FeCr_2O_4$, NiO, $(Cr, Fe)_2O_3$, and $NiMoO_4$. The phases determined in the scale formed on the CO side are Cr_3C_2 and Cr_2O_3. These results indicate that the oxidation process of J1 in air is different from that in CO.

Table 3 lists the oxide and carbide phases identified by XRD on the J5 and Fe-22Cr samples after the experiment. Although both materials are chromia formers, chromium carbide phase Cr_7C_3 was

found on the surface of only the Fe-22Cr sample exposed to CO side. For the J5 sample, chromia and $(Mn, Cr)_3O_4$ are present on both sides of the sample. However, $NiMoO_4$ is present only on the side exposed to the air

.

TABLE 3
XRD RESULTS OF OXIDE AND CARBIDE PHASES IDENTIFIED ON J5, AND Fe-22Cr AFTER EXPOSURE TO A DUAL AIR/CO ENVIRONMENT AT 750 ºC FOR 200 h

Alloy	Air	CO
J5	$(Mn, Cr)_3O_4$; $NiMoO_4$; Cr_2O_3	Cr_2O_3; $Mn_{1.5}Cr_{1.5}O_4$
Fe-22Cr	$Cr_{1.3}Fe_{0.7}O_3$; $MnFe_2O_4$	$Cr_{1.3}Fe_{0.7}O_3$;Cr_7C_3; $MnFe_2O_4$

Generally, the oxidation process in air by oxygen[8,9,15] proceeds according to reaction (6):

$$xM^{(s)} + 0.5yO_2^{(g)} \rightarrow M_xO_y^{(s)} \quad (6)$$

while the oxidation process in CO[9] proceeds according to reaction (7):

$$xM^{(s)} + yCO^{(g)} \rightarrow M_xO_y^{(s)} + yC^{(s)} \quad (7)$$

Literature data indicate that C may diffuse and dissolve in the alloy. If the alloy contains elements that form stable carbides, then formation of carbides may occur in this region. Since chromium carbides are stable, it is not surprising that they were found in J1 and Fe-22Cr after exposure to CO at 750 ºC for 200 h.

Figure 2 shows an SEM (backscattered electrons) cross-section micrograph for the CO side of J1. The scale formed on the surface appears to be relatively thick. It consists of outer and inner layers. The WDX analysis of the outer layer revealed that the layer is rich in Cr, whereas the inner layer is rich Ni. Also, there are dark areas that contain carbon and some Cr. This may indicate formation of a carburizing zone containing carbide precipitates which were also detected by XRD. Literature data show that carburizing zones were found in Ni-20%Cr exposed to CO.[9] It is worth noting that according to the XRD data shown in Table 3 spinel phases are not present in this scale.

Figure 3 shows an SEM (backscattered electrons) cross-section micrograph for the CO side of J5. The scale is uniformly distributed on the surface. It consists of outer and inner layers. There are bright-looking internal layers as well as non-continuous small dark areas. The WDX analysis revealed that the outer scale layer is rich in Mn, Cr, and oxygen. This could indicate the presence of $Mn_{1.5}Cr_{1.5}O_4$ spinel found by XRD. The inner layer is rich in Cr. This may indicate the presence of chromia as identified by XRD. The bright internal layer is rich in Mo and Ni. The dark areas are rich in Al and are free of carbon. This indicates that the carburization process did not take place. It appears that the scale containing (Mn, Cr) spinel may have served as a barrier for carbon diffusion during the experiment. It is possible that Mn plays a very important role in preventing formation of the carburizing zone.

Figure 4 shows an SEM (backscattered electrons) cross-section micrograph for the CO side of Fe-22Cr. It appears that Cr_2O_3 is dispersed in the scale under Fe-Cr spinel. Also, along a grain boundary, a carburizing zone formed. The WDX analysis revealed the presence of Cr (11.89 at.%), Fe(49.02 at.%) and C (37. 96) in a spot inside the carburizing zone. The XRD analysis revealed the presence of a chromium carbide-like phase. Also, literature data indicate possible formation of chromium carbide precipitates in the alloys that form protective Cr_2O_3 scales.[8]

Table 4 lists the scale thickness values for the CO side and the air side of the J1 and J5 samples.

TABLE 4
SCALE THICKNESS ON J5, AND Fe-22Cr AFTER EXPOSURE TO DUAL AIR/CO AT 750ºC FOR 200 h

	Scale Thickness, µm	
Alloy	**CO**	**Air**
J1	0.88 ± 0.04	2.51 ± 0.18
J5	1.59 ± 0.04	2.93 ± 0.16

The scales formed on the investigated materials in carbon oxide at 750ºC after 200 h are thinner in comparison to those formed in air. Taking into account the considerably lower chemical potential of oxygen in carbon oxide, it is not surprising that the scales are thinner in the CO environment. However, the scales on the CO side of the alloys are relatively thick. At present, mechanisms of corrosion reactions in CO are not fully known and are being studied.

FUTURE RESEARCH

Studies of materials performance for SOFC interconnect applications of ARC experimental and commercial nickel-based alloys and ferritic steel in dual environments of in moist air/CO are in progress. Experiments are planned for moist fuel and oxidizing environments as well as fuel environments containing sulfur compounds. Also, studies of the corrosion behavior of selected nickel-base alloys and stainless steels are in progress for balance-of-plant applications.

CONCLUSIONS

- Investigations of the J1, J5, and Fe-22Cr surfaces after exposure to the dual air/CO environment for 200 h at 750 ºC show different topography, microstructure, and phase formation of the scale formed on the air side from the scale formed on the CO side. This indicates that the corrosion processes in air and CO are different.

- For J1 and Fe-22Cr exposed to CO, XRD results determined the presence of a chromium carbide –like phase and the SEM investigations revealed the presence of carburizing zones. This indicates a detrimental effect of CO on the corrosion resistance of these materials.

- For the J5 exposed to CO, XRD results determined the presence of a protective $Mn_{1.5}Cr_{1.5}O_4$-like phase and the SEM investigations did not reveal the presence of carburizing zones. This indicates that the Mn, Cr spinel may have served as a barrier for diffusion of carbon.

ACKNOWLEDGEMENTS

The authors would like to thank Dr. David Alman and Dr. Paul Jablonski for developing and providing Ni-based alloys; Mr. Dan Davis for engineering support; Mr. Keith Collins, Mr. Steve Matthes, Mr. Richard Chinn, and Mr. David Smith of the U.S. Department of Energy, Albany Research Center, for their analytical support.

REFERENCES

1. L.Carrette, K.A. Friedrich and U. Stimming "Fuel-Cells-Fundamentals and Applications," Fuel Cells, 2001, 1, p. 5
2. Fuel Cell Handbook, fifth edition, U.S. Department of Energy, Office of Fossil Energy, National Energy Technology Laboratory
3. T.A. Czuppon, S.A. Knez, D.S. Newsome, Chemical Technology, 4th Ed., Vol. 13, p. 845
4. Fuel Cells, Opening New Frontiers in Power Generation, U.S. Department of Energy, Office of Fossil Energy, Federal Energy Technology Center
5. D.M. England and A.V. Virkar, J. ElecChem Soc. 148 (4) A330 (2001)
6. M. Ziomek-Moroz, G.R. Holcomb, B.S. Covino, Jr., S.J Bullard, D. E. Alman and P.D. Jablonski, "Corrosion Performance of Nickel -based Alloys and Ferritic Stainless Steels in Simulated Solid Oxide Fuel Cell Environments," 2005 Fuel Cell Seminar, November 14-18, 2005, Palm Springs, California
7. Z. Zhing, K. Natesan, Solid State Ionics 167 (2004) 9-16
8. N Briks and G H Meier "Introduction to High Temperature Oxidation of Metals," Edward Arnold (Publishers) Ltd, London 1983
9. S. Mrowiec and T. Werber, "Gas Corrosion of Metals," The Foreign Scientific Publications Department of the National Center for Scientific, Technical and Economic Information, for the National Bureau of Standards and the National Science Foundation, Washington, D.C., Warsaw, Poland 1978
10. R. Yamamoto, Y. Kadoya, H. Kawai, R. Magoshi, T. Noda, S. Hamano, and S. Isobe, " New Wrought Ni-Based Superalloys with Low Thermal Expansion for 700C Steam Turbines," Materials of Advanced Power Engineering-2002, Proc. 7th Liege Conf., Sept 30-Oct 3, 2002, Energy and Technology Vol. 21, Forschungszenitium Julich Gombh Inst. Fur Wekstoffe and Verfahren der Energietechik
11. R. Yamamoto, Y. Kadoya, S. Ueta, T. Noda, R. Magoshi, S. Nishimoto, T. Nakano, "Development of Wrought Ni-Based Superalloy with Low Thermal Expansion for 700C Steam Turbines, Fourth International Conference on Advances in Materials Technology for Fossil Power Plants, p. 442, October 25-28, 2004, Hilton Head Island, SC
12. D. E. Alman , P. D. Jablonski, "Low Coefficient Of Thermal Expansion (CTE) Nickel Base Alloys for Interconnect Applications In Intermediate Temperature Solid Oxide Fuel Cells (SOFC)," Superalloys 2004, edited by K. A. Green, T. M. Pollack, H. Harada, T.E. Howson, R.C. Reed, J. Schirra, and S. Walston, TMS 2004, p. 617
13. D. E. Alman, P. D. Jablonski, "Development of Low Coefficient Of Thermal Expansion (CTE) Nickel Alloys for Potential Use as Interconnect in Solid Oxide Fuel Cells," Fuel Cell Seminar, San Antonio, TX, November 2004
14. M. Ziomek-Moroz, S.D. Cramer, G.R. Holcomb, B.S. Covino Jr., S.J. Bullard, and P. Singh," Corrosion of Stainless Steel in Simulated Solid Oxide Fuel Cell Interconnect Environments," CORROSION 2005, Paper 05451
15. P. Kofstad "High Temperature Oxidation of Metals," John Wiley & Sons, Inc, New York 1966

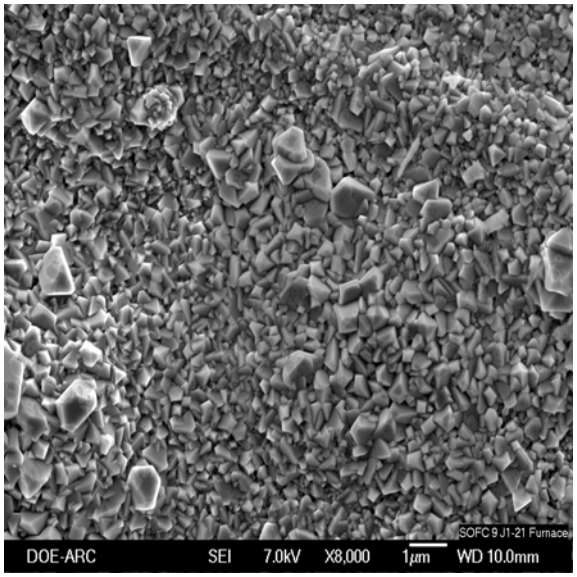

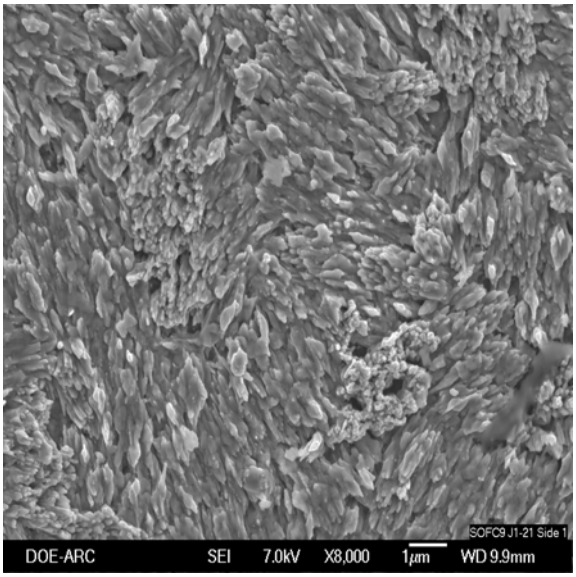

Air; XRD: $\underline{FeCr_2O_4}$, NiO; $(Cr, Fe)_2O_3$; $NiMoO_4$ **CO;** XRD: Cr_3C_2; Cr_2O_3

FIGURE 1- SEM micrographs (secondary electrons) and XRD results of J1 after exposure to a dual air/CO environment for 200h at 750°C.(Spinel phases)

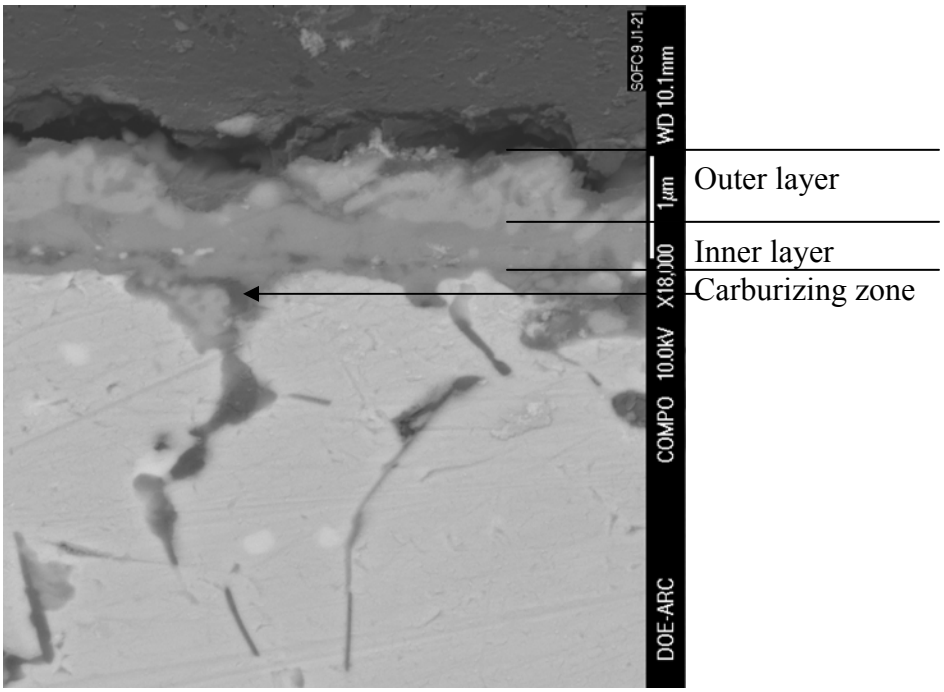

FIGURE 2- SEM (backscattered electrons) cross-section micrograph of the CO side of J1 after exposure to a dual air/CO environment for 200 h at 750°C.

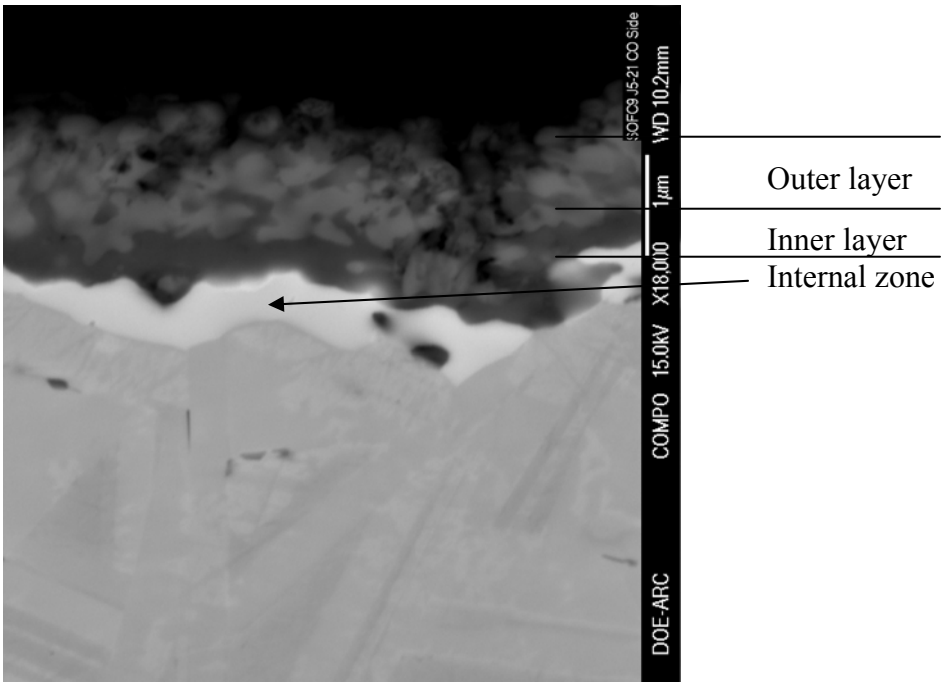

FIGURE 3- SEM (backscattered electrons) cross-section micrograph of the CO side of J5 after exposure to a dual air/CO environment for 200h at 750°C.

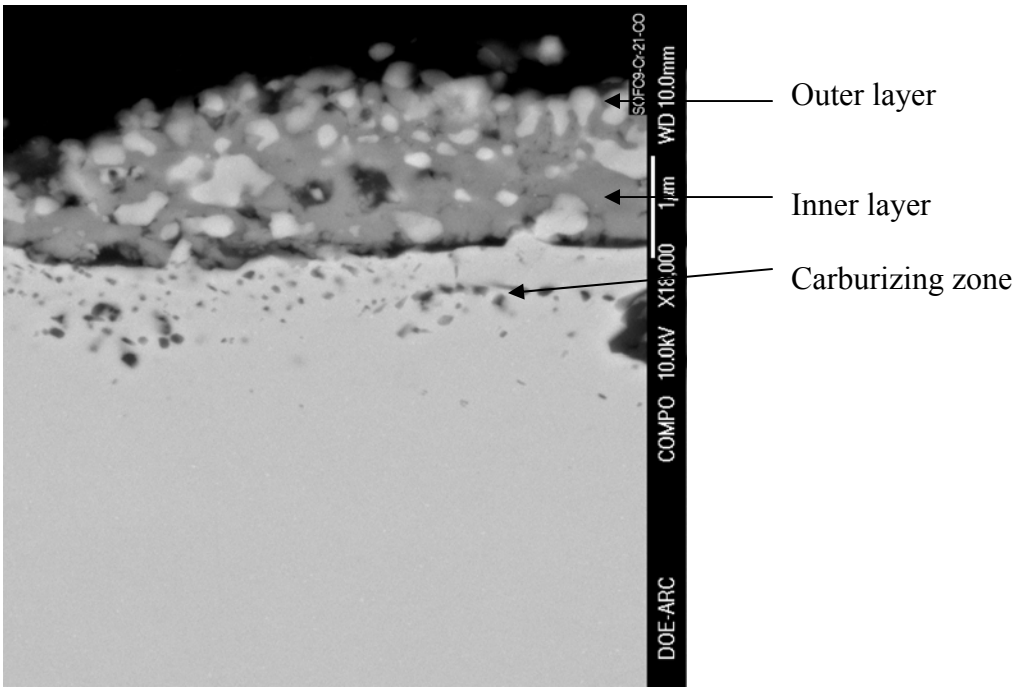

FIGURE 4- SEM (backscattered electrons) cross-section micrograph of the CO side of Fe-22Cr after exposure to a dual air/CO environment for 200h at 750°C.